Iraqi Journal of Nanotechnology
synthesis and application
Journal Homepage : https://publications.srp-center.iq/index.php/ijn

Dityrosine Crossed-linked Amyloid-like Fibrils as Bionanomaterials

Youssra K. Al-Hilaly[1,2*], Mahmoud B. Maina[2,3], Alaa Abdul-Sada[4], Louise C Serpell[2*]

1- Chemistry Department, College of Science, Mustansiriyah University, Baghdad, Iraq,
2- Dementia Research group, Sussex Neuroscience, School of Life Sciences, University of Sussex, Falmer, UK
3- College of Medical Sciences, Yobe State University, Nigeria.
4- Department of Chemistry, School of Life Sciences, University of Sussex, Falmer, UK
*Corresponding author: Louise C Serpell email: L.C.Serpell@sussex.ac.uk , Youssra Al-Hilaly email: youssra.alhilaly@uomustansiriyah.edu.iq

Keywords:
Dityrosine cross-link; Metal-catalysed oxidation; Bionanomaterials; Functional amyloid-like fibrils

Abstract

Bionanomaterials have great potential for applications in tissue engineering and regenerative medicine. Recently, amyloid-like fibrils have been used in bionanomaterials preparation due to their stability and biocompatibility. Covalent dityrosine bond formation has been identified as a useful tool in the design of such bionanomaterials. In this study, two short amyloidogenic peptides containing tyrosine residues with the amino acid sequence HYFNIF and VIYKI, were used as a model system to investigate the effect of oxidation and their ability to form dityrosine cross-links. Using a range of biophysical techniques, we showed that both HYFNIF and VIYKI form dityrosine cross-linked fibrils using copper-catalysis, and phosphate buffer is more efficient in dityrosine formation. Dityrosine forms more rapidly in VIYKI fibrils compared to HYFNIF due to the fibrillar architecture. Dityrosine cross-linked HYFNIF and VIYKI fibrils could be useful to prepare bionanomaterials.

Introduction

Many studies have shown the utility of bionanomaterials in biomedical applications, such as regenerative medicine. These materials must be biocompatible, porous, mechanically tunable, biodegradable, easily prepared, and similar to a native cell or tissue [1, 2]. To provide some of these properties, multiple cross-linking approaches have been used in the design of bionanomaterials [3, 4] such as UV irradiation, dehydration, and chemical techniques, such as glutaraldehyde cross-linking have been used [5]. Two tyrosine residues crosslink to form dityrosine via carbon-carbon covalent bond and dityrosine has been identified as a useful tool in the design of such bionanomaterials [3]. Dityrosine is particularly interesting for bionanomaterial stabilisation because of its *in vivo* relevance as it has been shown as a cross-linker in anthropods, where it helps to stabilise resilin through the formation of a stable three-dimensional network [6]. It has been shown in several elastic and structural proteins including elastin, fibroin, keratin, cuticlin, and collagen [7-10], where it contributes to tuning the mechanical strength and subsequently the insolubility of these proteins [11]. Dityrosine also serves a protective role in proteins [12, 13]. In Ascaris suum it forms part of the structural components of the cuticle [14], and it is involved in the hardening of mosquito egg chorion [15]. In addition, dityrosine is also relevant in the context of diseases and ageing. It has been shown in amyloid plaques and lipofuscin in Alzheimer's disease [16, 17], Lewy bodies in

 DOI: https://doi.org/10.47758/ijn.vi1.23

Parkinson's disease [18], and cataracts in the eye lens [19, 20]. The involvement of dityrosine in these amyloid diseases also highlights its importance towards understanding the working mechanism and function of functional amyloids.

To study dityrosine formation and its application to the rational design of bionanomaterials, and its relevance in functional and pathological amyloids, here, the short amyloidogenic peptides; HYFNIF and VIYKI were used as model systems. The HYFNIF is a sequence from human bloom syndrome protein and VIYKI from Drosophila chorion protein identified via the Waltz algorithm [21] and structurally validated using biophysical techniques, including transmission electron microscopy (TEM), linear dichroism (LD), circular dichroism (CD) spectroscopy and X-Ray Fiber Diffraction (XRFD) [21, 22]. Biophysical studies with short amyloidogenic peptides are particularly relevant for the development of bionanomaterials. Understanding their behaviors enables the production of new functional nanoscale materials with applications in nanotechnology and biomaterials [23]. This is especially due to their self-assembly properties that leads to very stable, ordered structures under diverse conditions, from liquid crystals to rigid nanotubes [24]. Functionalised amyloid-like fibrils with Lewis-acid-like catalytic activity were prepared from HYFNIF peptide and heterometallic Zn_2Dy_2 complex [25]. Using HYFNIF and VIYKI peptides as a model, atomic force microscopy (AFM) has been used to provide structural basis of polymorphism within amyloid populations [26]. Both peptides contain single tyrosine (Y) each which can participate in intermolecular dityrosine cross-linking. Thus, they provide excellent model systems for investigating the structural and chemical properties of amyloids covalently cross-linked with dityrosine. Studying dityrosine cross-linking in small peptide models can enhance our understanding of dityrosine's role in the folding and assembly of other physiologically relevant peptides and proteins such as Aβ and α-syn, as well as, in the design of biomaterials. Here, fibrils produced from VIYKI peptide appeared to have a greater ability than HYFNIF fibrils to oxidise and form dityrosine cross-links which suggest that the preformed VIYKI fibrils can enhance dityrosine formation by bringing two tyrosine residues in close contact for covalent cross-linking. In contrast, the tyrosine residues in the HYFNIF fibrils are oriented away from one another, and as a consequence, dityrosine formation is more restricted. The data also revealed that the pH of the oxidation environment, combined with the peptide net charge strongly influences the level of dityrosine formation. Given the stability of dityrosine cross-links, this finding will support future studies on these and similar peptides in the design of self-assembling peptides and bionanomaterials.

Materials and Methods

Preparation of Waltz peptide fibrils

The two lyophilised HYFNIF and VIYKI peptides capped with N-terminal acetylation and C-terminal amidation were purchased at 95% purity as TFA salts (JPT peptide Technologies, Germany). Lyophilised peptides were dissolved in Milli-Q water filtered through a 0.22 μm filter and incubated at a concentration of 1 mg/ml for both HYFNIF and VIYKI for one week at room temperature to generate amyloid-like fibrils. TEM negative staining was used to confirm fibril formation. The stock solutions of the fibrils were stored in the dark at room temperature until required.

Copper-catalysed dityrosine cross-linked HYFNIF and VIYKI fibrils at neutral pH

HYFNIF and VIYKI fibrils were diluted in 0.22 μm filtered Milli-Q water to a final concentration of 0.1 mM. The diluted fibrils were incubated with $CuCl_2$ (0.1 mM) and H_2O_2 (2.5 mM) at 37 °C with agitation at 300 rpm for 72 h. To monitor dityrosine formation, the fluorescence spectra were recorded over 72 h as described in fluorescence methods.

Tyrosine and dityrosine fluorescence

Varian Cary Eclipse fluorescence spectrophotometer (Varian Ltd., Oxford, UK) was used for fluorescence measurements using a single cell peltier accessory set at 21 °C. Signals were collected using 1 cm path length quartz cuvette (Starna, Essex, UK). Dityrosine fluorescence was monitored with an excitation wavelength of 320 nm, and emission spectra were collected between 340 and 500 nm, with the maximum dityrosine fluorescence at around 410 – 420 nm. The tyrosine fluorescence signal was monitored with an excitation wavelength of 280 nm and emission collected at 305 nm. 10 nm excitation and emission slits were used, with 300 nm/min scan rate, 2.5 nm data intervals, and an averaging time of 0.5 s. The photomultiplier tube detector voltage was set at 500 V.

Negative stain TEM

A total of 4 µl of each fibril sample was pipetted on a Formvar/carbon-coated 400-mesh copper grid (Agar Scientific, Essex, UK). After 1-2 min incubation, excess solution was removed from the grid using filter paper. Next, the grid was washed with 4 µl filtered Milli-Q water, blotted with a filter paper and stained by the addition of 4 µl of filtered 2% (w/v) uranyl acetate. After 1 min incubation, the grid was blotted using a filter paper and allowed air-dry before examination on a Hitachi 7100 transmission electron microscope (Hitachi, Germany). The TEM was fitted with a Gatan Ultrascan 1000 CCD camera (Gatan, Abingdon, UK) and images collected at an operating voltage of 100 kV.

Circular dichroism spectroscopy

The conformations of the non-oxidised and copper-catalysed dityrosine cross-linked HYFNIF and VIYKI fibrils were detected by CD. Far and near UV CD spectra were recorded either in water or in 12.5 mM phosphate buffer at pH 7.4, using Jasco J-715 spectropolarimeter (Jasco UK, Great Dunmow, UK) connected to a peltier temperature control system. All spectra were recorded at 21°C with a continuous scan at a pitch of 0.1 nm and a scan rate of 50 nm/min (response time 4 sec, slit width 1 nm). The spectra were recorded between 180 - 320 nm by averaging triplicate scans and corrected by subtracting the averaged triplicate scans of blank buffer spectra. Quartz demountable cuvettes (Starna Scientific Ltd) were used to collect the CD spectra, and generally, the path lengths were between 1- 0.1 mm to obtain better spectra with a high-tension voltage (HT [V]) of > 600. Raw data was processed and converted into molar ellipticity (degree.cm^2. dmol^{-1}) using the following equation:

$$\theta\ (\text{deg.cm}^2.\text{dmol}^{-1}) = 100.\ \theta\ (\text{mdeg}) / c\ (\text{M}).\ l\ (\text{cm})$$

Where l is path length in cm, c is the molar concentration of the sample in mole/L, and θ is ellipticity reading in mdeg.

Linear dichroism artifact identification

Detection of Linear dichroism artefacts, which arise from the orientation effects of fibrils, was investigated by placing the cuvette close to the detector and recording CD spectra after rotating the cuvette 0° and 90°.

Sample preparation for LC-ESI MS/MS analysis

Copper-catalysed dityrosine cross-inked HYFNIF (0.1 mM) and VIYKI (0.05 mM) fibrils were prepared in water and then lyophilised using a Modulyo 4K Freeze Dryer (Edwards, Crawley, England). The lyophilised fibrils were hydrolysed using evacuated sealed tubes under acidic conditions of (6 M) HCl, 10% TFA, and 1% phenol at 110 °C for 48 h. They were then dried under nitrogen gas, dissolved in 100 µl of 0.1% formic acid in water and filtered using a Millipore 0.22 µm filter into a 0.2 ml tube.

Detection of dityrosine by LC-ESI MS/MS

A total of 20 µl of dityrosine cross-linked HYFNIF and VIYKI fibrils hydrolysate were injected on to a Phenomenex Gemini 3u C_6–phenyl 110 (150 mm x 4.6 mm, 3 micron) column using an HPLC system (Waters Alliance 2695, Ireland) coupled to the mass spectrometer (Quttro Micro Premier, triple quadruple mass spectrometer, Waters, Ireland) operated in the MRM mode with positive ESI. The mobile phase solvents were A: 0.1% formic acid in water; and B: 0.1% formic acid in acetonitrile. The gradients were as follows: t = 0 min, 0% B; t = 1 min, 0% B; t = 15 min, 100% B; t = 20 min, 100% B; t = 25 min, 0% B; t = 30 min, 0% B, and the flow rate was 200 µl/min. Mass spectrometric detection was performed by positive ion ESI tandem mass spectrometry on a triple quadrupole mass spectrometer. Argon was used as the collision gas (Argon) at 5.95e^{-}003 mbar at 26 ev collision energy. The conditions for the mass spectrometer were as follows; ESI voltage 3 kV, the cone voltage 35 V, the source temperature was 100 °C, and the desolvation temperature was 400 °C and 300 L/h flow rate of nitrogen gas.

Exploring the effect of the pH and buffer type on dityrosine cross-link formation

To investigate the effect of the pH and buffer type on dityrosine cross-link formation in both HYFNIF and VIYKI fibrils, 0.1 mM HYFNIF and 0.1 mM VIYKI fibrils were incubated respectively with $CuCl_2$ using 1:1 molar ratio and 2.5 mM H_2O_2 in a) 50 mM phosphate buffer pH 7.4 and b) 50 mM HEPES buffer pH 7.4 and the oxidation reactions were performed at 37 ºC with agitation at 300 rpm for 26 h. Dityrosine formation was monitored by fluorescence and the spectra were recorded over 26 h.

Oxidation of HYFNIF and VIYKI fibrils for circular dichroism studies

(a) HYFNIF and VIYKI fibrils were diluted in water to a final concentration of 1 mg/ml and incubated in the presence of $CuCl_2$ at a molar ratio of 1:1 ($CuCl_2$/peptide) and (H_2O_2 (28.3 mM) and (37.0 mM) respectively. The oxidation reactions were performed at 37 ºC with the agitation of 300 rpm for 72 h. circular dichroism spectra were recorded as explained in circular dichroism measurement using a 0.1 mm path length cuvette.
(b) 0.25 mM of VIYKI fibrils was oxidised using $CuCl_2$ (250 µM) and H_2O_2 (6.25 mM) in 12.5 mM phosphate buffer at 37 ºC with agitation at 300 rpm for 72 h. CD spectra were recorded every 24 h.

Immunogold labelling negative stain TEM

Dityrosine cross-linked HYFNIF and VIYKI fibrils were prepared in 12.5 mM phosphate buffer and immunogold labelled 'on grid' for dityrosine using a well described protocol [27]. A modified phosphate-buffered saline (called PBS+) was used for all dilutions and washes. Briefly, 4 µl aliquots of the fibrils were placed onto Formvar/ carbon coated 400 mesh copper support grids, left for 1 min, then blotted with a filter paper. The grids were next blocked in normal goat serum (1:10) for 15 min at room temperature and incubated with (10 µg/ml) mouse dityrosine monoclonal antibody (Japan Institute for the Control of Aging JaICA, Shizuoka, Japan) for 2 h at room temperature. The grids were next washed three times for two min with PBS+, and then immunolabelled in a 10 nm gold nanoparticle-conjugated goat anti-mouse IgG secondary probe (BBI solution Ltd, UK, 1:10 dilution) for 1 h at room temperature. After 5x2 min PBS+ and 5x2 min distilled water rinses, the grids were negatively stained as described in the TEM negative staining section.

Results

Using VIYKI and HYFNIF as models for preparing functional amyloid-like fibrils

Two amyloidogenic peptides previously characterised using WALTZ algorithm, VIYKI and HYFNIF [22] were selected as simple amyloid models to better understand dityrosine formation at a structural level due to their highly organised fibrillar structure and the positions of the tyrosine residues allowing for potential dityrosine formation Figure 1.

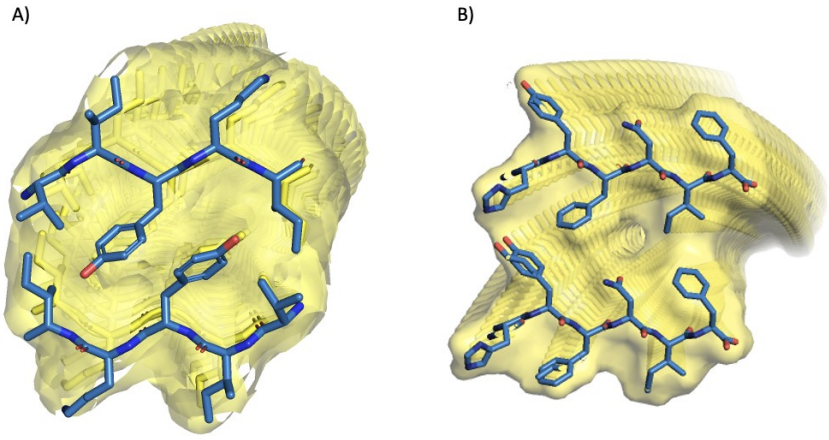

Figure 1 Structural models of protofibres formed from the two Waltz peptides, VIYKI and HYFNIF. Predicted models of amyloid protofibres made from a) VIYKI and b) HYFNIF. These models were generated and validated by comparing simulated and experimental XRFD data as described in [22].

Characterization of VIYKI and HYFNIF amyloid-like fibrils

VIYKI and HYFNIF form amyloid-like fibrils in water and have been previously studied using TEM, CD, LD, and XRFD (Morris et al., 2013). Here, the VIYKI and HYFNIF peptides were dissolved in water at a concentration of 1mg/ml and allowed to assemble to fibrils at room temperature for 7 days. TEM negative staining confirmed the expected long straight unbranching amyloid-like fibrils. Both peptides assembled to form laterally associated protofilaments and twisted morphologies (Figure 2, A and B). Tyrosine fluorescence spectra of the preformed amyloid-like fibrils at a concentration of 100 µM revealed a strong peak at 305 nm, characteristic of the fluorescence arising from tyrosine residues (Figure 2, A and B). Comparison of the signal intensity arising from the two peptides revealed a significantly stronger signal (a.u. ~125) for fibrils formed by VIYKI compared to HYFNIF (a.u. ~ 40). This may reflect differences in the arrangements of the peptides within the fibrils and the exposure/burial and axial stacking of the tyrosine residues.

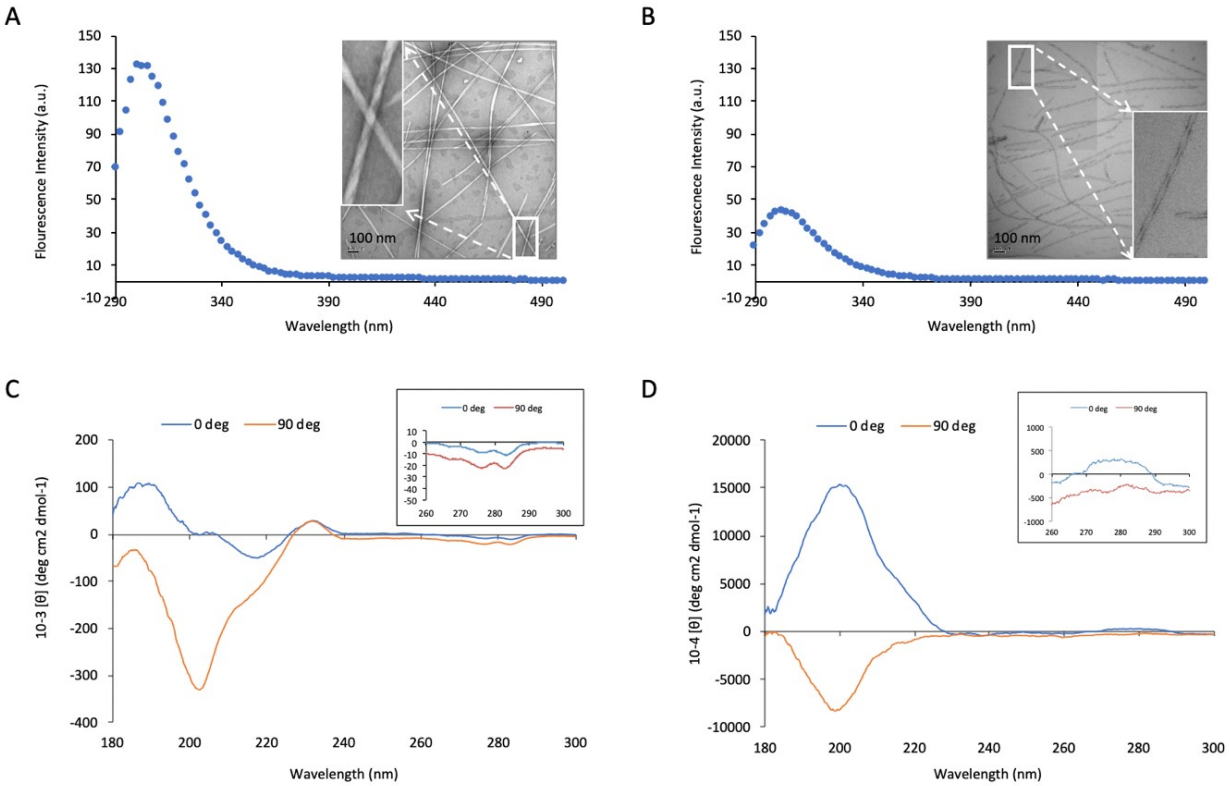

Figure 2 Structural characterisation of amyloid-like fibers. Tyrosine fluorescence spectra and transmission electron microscopy images of A) VIYKI amyloid-like fibrils and B) HYFNIF amyloid-like fibrils in the water at a concentration of 100 µM. Upon excitation at 280 nm the tyrosine residue results in a peak at 305 nm. CD and LD spectra of C) VIYKI fibrils and D) HYFNIF recorded by positioning the cuvette at 0 and 90 deg, showing the inversion the signal at 200 nm which is attributed to the artefactual LD signal. The upper panel inset shows that the signal arising from contribution of tyrosine residues does not invert by positioning the cuvette at 90 deg.

To detect the conformation of VIYKI and HYFNIF amyloid-like fibrils, the CD spectra of 1mg/ml VIYKI and HYFNIF were recorded (Figure 2, C and D). The CD spectra of HYFNIF and VIYKI fibrils showed features that were unlike commonly observed spectra shown for cross-β rich amyloid fibrils. Although a classic β-sheet conformation shows a typical signal at ~ 195 (positive) and ~ 218 nm (negative), HYFNIF and VIYKI fibrils exhibited slightly shifted signals (Figure 2, C and D). VIYKI fibrils exhibited a negative signal maximum at 218 – 220 nm (Figure 2, C) that corresponds to the negative β-sheet signal. On the other hand, a positive maximum signal at 200 nm was observed in CD spectra of both HYFNIF and VIYKI fibrils, which could be attributed to an artefactual LD signal. Additionally, two signals arising from tyrosine were observed at 275 and 235 nm. The signal at 275 nm split into two peaks at 276 and 282 nm and was taken to arise from electron coupling of the tyrosine residues indicating proximity of tyrosines within the amyloid-like fibril structure [22, 28].

To test if the signal at 200 nm is arising from the artefactual LD signal, CD spectrum was recorded by positioning the cuvette at 90 deg, and showing the inversion signal at 200 nm which in turn indicates the orientation dependent of this signal (Figure 2, C and D).

Copper-catalysed dityrosine formation at neutral pH

Preformed amyloid-like fibrils (0.1 mM) HYFNIF and (0.1 mM) VIYKI were incubated for 72 h with $CuCl_2$ at 1:1 molar ratio and (2.5 mM) H_2O_2 in water (pH of 5.0 and 6.1 respectively) at 37 °C with agitation at 300 rpm. Dityrosine formation was detected by tyrosine fluorescence, and it shows a signal at 410 nm (Figure 3, A and B) and a decline in the intensity of the in the tyrosine signal at 305 nm.

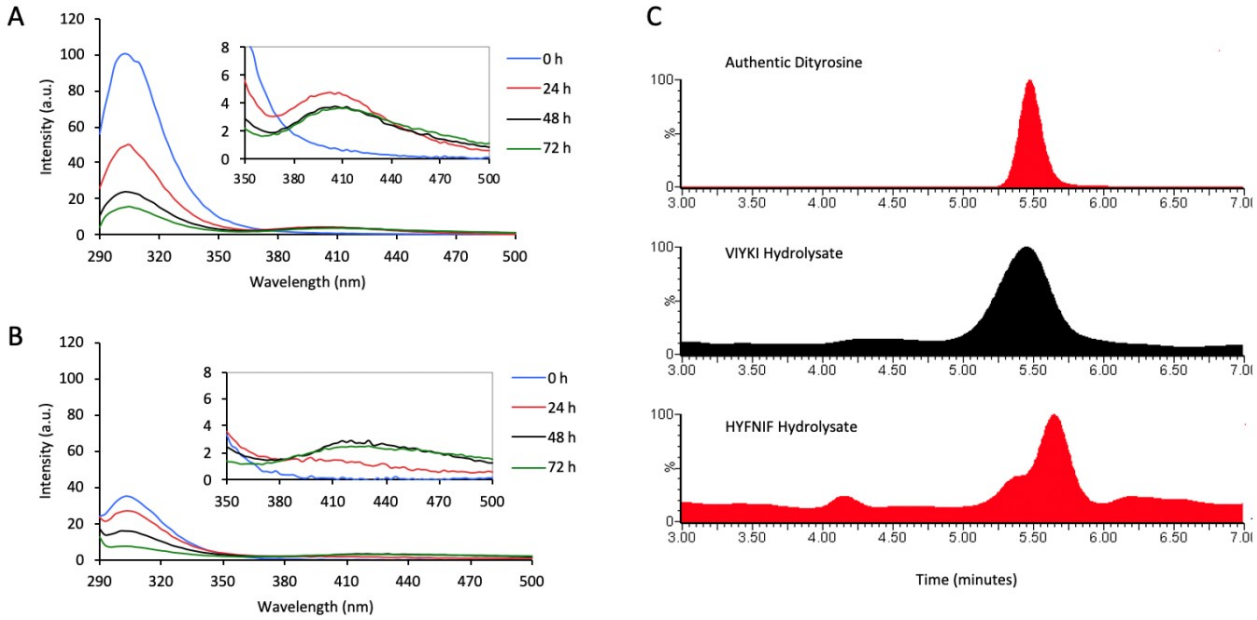

Figure 3 Dityrosine identification using tyrosine fluorescence and mass spectrometry. 0.1 mM of (A) VIYKI and (B) HYFNIF fibrils were incubated in the presence of $CuCl_2$/ H_2O_2 in water for three days at 37 °C with agitation of 300 rpm and dityrosine formation was recorded by tyrosine fluorescence. The insets showing dityrosine fluorescence signal arising at 410 nm. C) LC-ESI MS/MS chromatograms recorded in the MRM mode for dityrosine from authentic dityrosine, VIYKI and HYFNIF fibrils hydrolysate. Oxidised VIYKI and HYFNIF fibrils were obtained from the incubation of 0.05 mM VIYKI and 0.1 mM HYFNIF fibrils with $CuCl_2/H_2O_2$ in water at 37 °C with agitation of 300 rpm.

To further confirm the dityrosine cross-links formation, hydrolysate from acidic hydrolysis of the oxidised VIYKI and HYFNIF fibrils was tested by LC-ESI MS/MS. The dityrosine formation was identified using transition reactions ions 361.1 315, the most intense transition reaction ion, and has a retention time of 5.5 min (Figure 3, C), consistent with that of authentic dityrosine.

Investigation of the conformational changes during dityrosine cross-links formation

CD spectra of oxidised HYFNIF and VIYKI fibrils were measured to gain insight into the effect of dityrosine cross-linking on the secondary and tertiary structures upon dityrosine formation. CD spectra of 1 mg/ml HYNIF fibrils and 1 mg/ml VIYKI fibrils before and after incubation with $CuCl_2/H_2O_2$ in water were recorded (Figure 4). CD showed interesting development in both near and far UV CD spectra of dityrosine cross-linked amyloid-like fibrils. Incubation of HYNIF fibrils with $CuCl_2/H_2O_2$ causes an appearance of a positive CD band at 190 nm, which is thought to be masked by the strong LD signal in the CD spectra of non-oxidised fibrils, and a negative signal 220 nm and is accompanied by a loss of positive LD band at 200 nm. These results suggest that oxidised fibrils have lost their ability to self-align and that may

be due to formation of dityrosine cross-linked fibrils, which prevents the lateral alignment that leads to LD artefacts (Figure 2, D). The near UV CD spectrum of non-oxidised VIYKI fibrils exhibits two prominent negative signals at 276 and 282 nm, which arise from tyrosine residues. Dityrosine cross-linked VIYKI fibrils showed a significant decline in tyrosine signals at 276 and 282 nm which may correspond to the loss of tyrosine residue due to tyrosine oxidation to form dityrosine crosslinks (Figure 4). CD spectra from dityrosine cross-linked amyloid-like fibrils are consistent with more commonly observed signatures for β-sheet structure and disappearance of the artefactual LD signal in the resulting CD spectra indicates less alignment of dityrosine cross-linked fibrils.

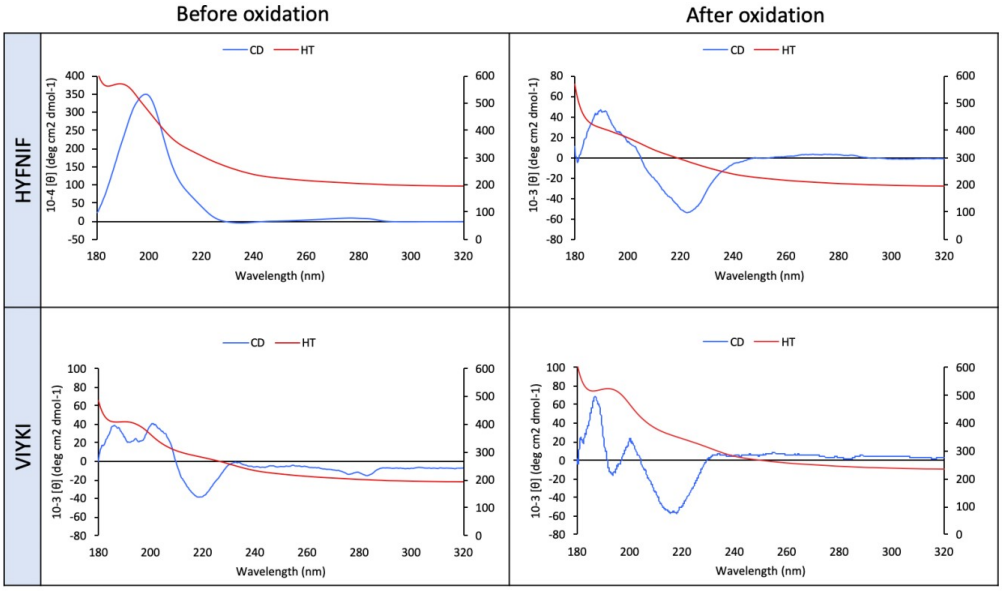

Figure 4 Structural development during dityrosine crosslink formation. CD spectra of 1 mg/ml HYNIF fibrils and 1 mg/ml VIYKI fibrils before and after incubation with $CuCl_2/H_2O_2$ in water. Incubation of the peptides with $CuCl_2/H_2O_2$ leads to loss of LD signal at 200 nm and increase in the β-sheet signals.

Optimization of dityrosine cross-link formation using two different buffers at pH 7.4

It has been shown that the copper ion coordination varies in different buffer conditions [29] and can form ternary complex with phosphate and precipitate as copper(II) phosphate. To optimise dityrosine formation and to explore the performance of the metal-catalysed oxidation system using different types of buffers, phosphate and HEPES buffers were used. VIYKI and HYFNIF fibrils (0.1 mM) were incubated with $CuCl_2/H_2O_2$ in two different buffers at pH 7.4 (50 mM HEPES buffer and phosphate buffer). The oxidation process was undertaken for 26 h at 37 ^oC, and dityrosine formation was monitored using an excitation wavelength of 320 nm (Figure 5 A and B). After 26 h oxidation, dityrosine signal intensity around 410 nm for VIYKI was (a.u. ~354) in phosphate buffer, while it was around (a.u. ~ 28) in HEPES buffer, which is about 12 times more in phosphate buffer (Figure 5, A iii). In the same manner, fluorescence data shows that HYFNIF fibrils form dityrosine in phosphate buffer better than in HEPES buffer (Figure 5, B iii). However, the results revealed that VIYKI fibrils exhibited more susceptibility to form dityrosine linkages than HYFNIF fibrils in both HEPES and phosphate buffer, and also more rapidly, as it took just 15 min to give a significant dityrosine signal in VIYKI fibrils (Figure 5, A ii), compared to the 2 h required to yield dityrosine in HYFNIF fibrils (Figure 5, B ii). In total, our results show that using phosphate buffer to perform the copper-catalysed oxidation process produces increased dityrosine formation in both HYFNIF and VIYKI peptides and that VIYKI fibrils form dityrosine linkage rapidly and more efficiently than HYFNIF. This could be attributed to the differences in the amino acid sequences of the amyloidogenic peptide and their structural architecture that affect their ability to produce dityrosine cross-links.

The morphology of the dityrosine cross-linked amyloid-like fibrils was visualised by electron microscopy and displayed a remarkable diversity (Figure 5, C). The TEM images of dityrosine cross-linked fibrils in phosphate buffer showed evidence of shortening of the VIYKI fibrils (49.0 – 863.0 nm) compared to those non-oxidised (1762.0 – 1855.0 nm), and

also clumping of short fibrils. Less fragmentation was observed after 26 h of oxidation in HEPES buffer (Figure 5, C), and that may reflect the extent of oxidation using different types of buffers. Similar to VIYKI fibrils, HYFNIF fibrils underwent fragmentation upon oxidation in phosphate buffer, but TEM images showed that after 26 h of oxidation in phosphate buffer both long and short HYFNIF fibrils were observed (Figure 5, C). The fluorescence results (Figure 5, B) revealed that HYFNIF fibrils have less ability to form dityrosine cross-links and this may result in the less affected morphology of oxidised HYFNIF fibrils. It is clear from the TEM micrographs of both dityrosine cross-linked HYFNIF and VIYKI fibrils in HEPES buffer that they underwent less fragmentation, and the main morphological change is that the fibrils became thicker and clumped together along the fibril length.

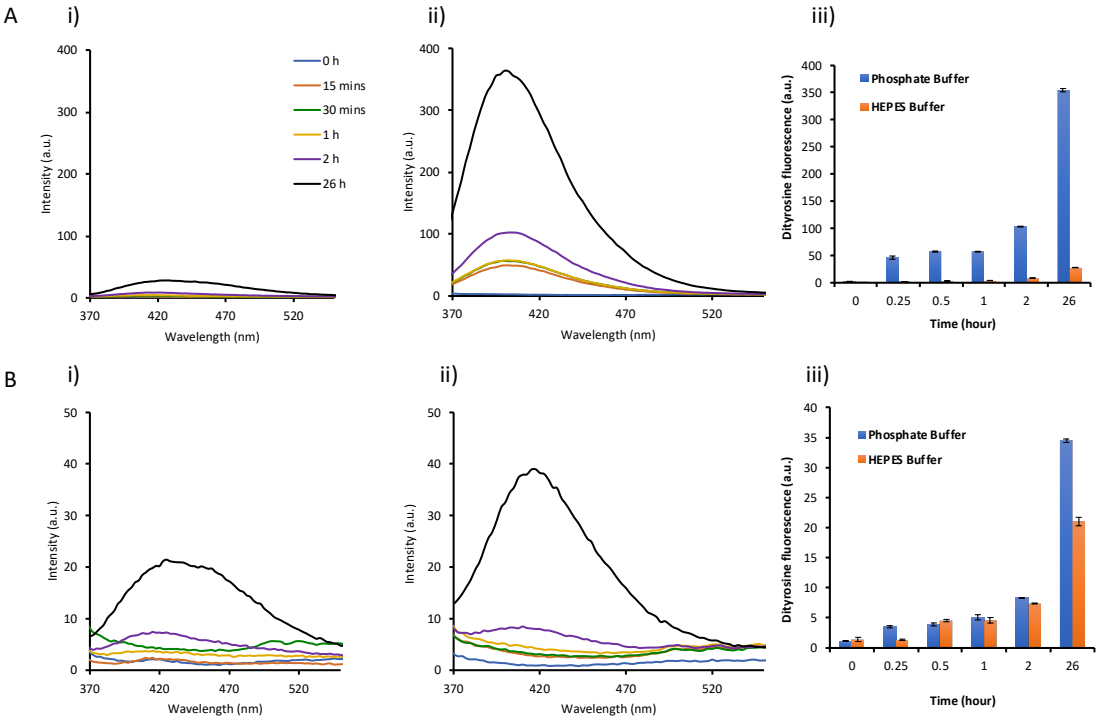

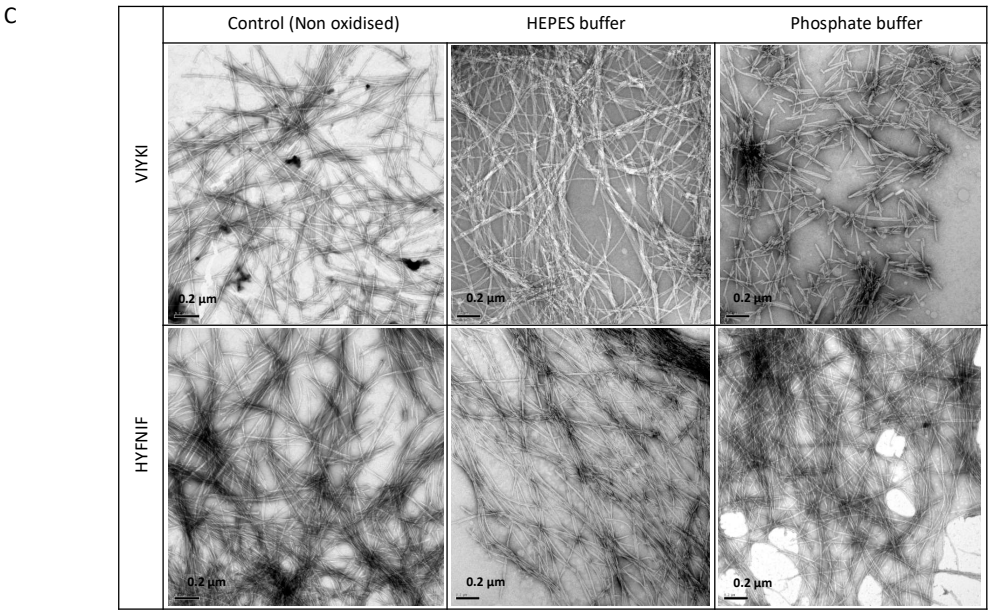

Figure 5 Copper-catalysed dityrosine cross-links formation at pH 7.4. (A) Oxidation of VIYKI fibrils in i) HEPES and ii) phosphate buffer respectively. B) Oxidation of HYFNIF fibrils in i) HEPES and ii) phosphate buffer respectively. Dityrosine formation was monitored using excitation wavelength of 320 nm. Copper-catalysed dityrosine formation in phosphate buffer was significantly higher compared to that in HEPES buffer (A, iii and B, iii). C) TEM micrographs of dityrosine cross-linked VIYKI fibrils and HYFNIF fibrils in HEPES buffer and phosphate buffer. While VIYKI fibrils underwent noticeable morphological changes upon oxidation in both HEPES and phosphate buffer, HYFNIF fibrils showed less changes especially in HEPES buffer.

As VIYKI shows more ability to form dityrosine cross-links in phosphate buffer, and to gain more insight into the conformational change for dityrosine cross-linked VIYKI fibrils, further CD experiments were performed to monitor changes in the main chain conformation of (0.25 mM) VIYKI fibrils during dityrosine cross-linking formation at pH 7.4 over 48 h. A significant decline in the intensity of the tyrosine signals at 275 nm and 235 nm was observed, indicating the loss of the tyrosine during the oxidation. Additionally, there was a significant increase in minima at 218 nm suggesting an increase in β-sheet content (Figure 6, A). No LD effect was observed after oxidation, indicating that the fibrils underwent a structural development upon oxidation that prevents fibrils from be aligned and consequently abolished the artefactual LD signal (Figure 6, B). The pH of the oxidation environment has a strong influence on the dityrosine production and that is due to the net peptide charge. Although the CD and TEM data of the oxidised fibrils revealed interesting structural and morphological changes upon the oxidation processes, no dityrosine characteristic signal was observed in CD.

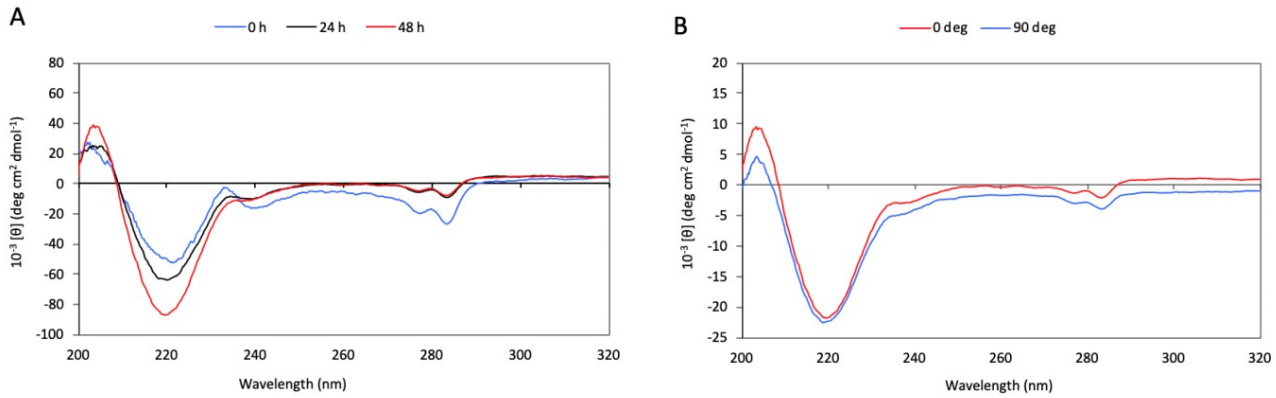

Figure 6 Conformational developments during dityrosine cross-links formation. A) CD spectrum development over oxidation of (0.25 mM) VIYKI fibrils in phosphate buffer, pH 7.4. B) LD effect was detected by collecting CD spectra of (0.1 mM) VIYKI fibrils after 48 h of oxidation in phosphate buffer, pH 7.4. The spectra were obtained by positioning the cuvette at 0 and 90 deg to the detector.

The distribution of dityrosine crosslinks on fibrils

To further detect the dityrosine cross-links, and show the dityrosine distribution in the oxidised fibrils, TEM immunogold labelling using a dityrosine specific monoclonal antibody was performed. Figure 7 shows labelling using an anti-dityrosine, gold-conjugated antibody on HYFNIF and VIYKI amyloid-like fibrils, revealing gold distributed close to the fibrils that were grown in an oxidising environment. Non-oxidised HYFNIF and VIYKI fibrils did not label with the dityrosine antibody. Very strong evidence of dityrosine identity was provided using these specific monoclonal dityrosine antibodies. Electron micrographs of oxidised VIYKI fibrils, which had been labelled with the gold-conjugated dityrosine antibody, revealed that dityrosine cross-links are distributed along the fibrils (Figure 7, A ii) suggesting that dityrosine coupling occurs within fibrils. Although fluorescence data showed that much higher dityrosine fluorescence intensity was generated in oxidised VIYKI fibrils (Figure 5, A), it is obvious that less gold labelling was observed in oxidised VIYKI fibrils (Figure 7, A ii) compared to oxidised HYFNIF fibrils (Figure 7, B ii), and this may support the view that dityrosine cross-link is formed internally within fibrils. Consequently, the dityrosine cross-link epitope is less accessible to bind the antibody. No labelling was observed for non-oxidised fibrils providing a strong evidence of dityrosine antibody specificity toward dityrosine versus tyrosine.

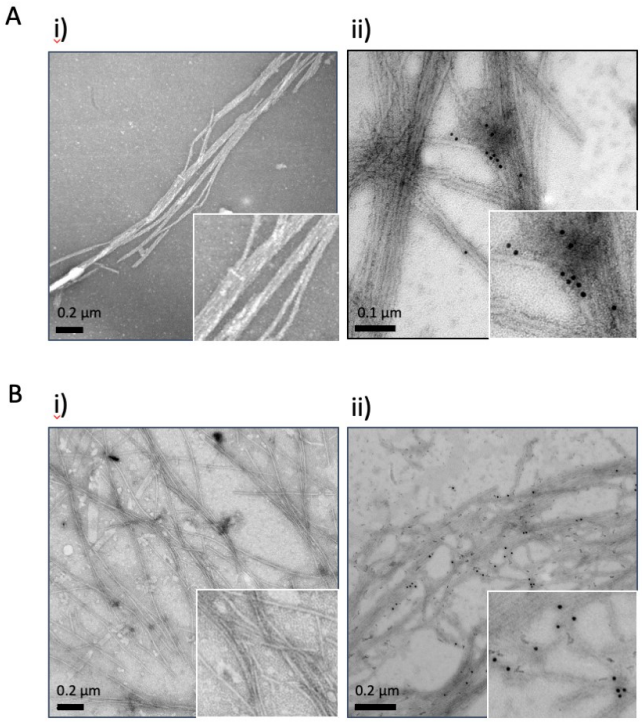

Figure 7 TEM immunogold labelling. A) VIYKI fibrils and B) HYFNIF fibrils immunogold labelled to detect dityrosine crosslinks before (i) and after (ii) oxidation. 0.1 mM VIYKI and HYFNIF fibrils were oxidised for 3 h using 0.1 mM $CuCl_2$ and 2.5 mM H_2O_2 in 50 mM phosphate buffer, pH 7.4. The oxidation process was undertaken at 37° C, and agitation 300 rpm. The immunogold labelling micrographs shows positive labelling for dityrosine in oxidised fibrils compared with non-oxidised fibrils that did not label with dityrosine antibody.

Data presented here, suggest that the phenol groups of tyrosine residues are in close proximity to one another in VIYKI fibrils and proximity may make the carbon–carbon covalent bonding easier than in HYFNIF fibrils in which the phenol groups were arranged further away from each other (Figure 8).

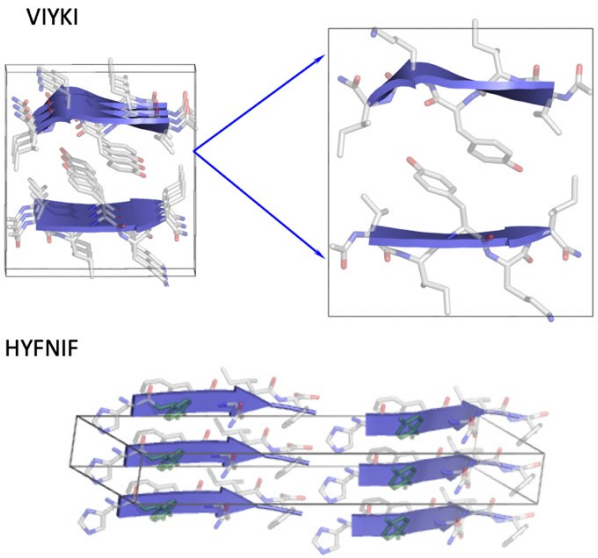

Figure 8. Proposed cell units of VIYKI and HYFNIF fibrils are determined from XRFD [22]. In VIYKI fibrils the phenol groups of tyrosine residues are orientated to be close enough to form dityrosine linkages. While, in HYFNIF the tyrosine residues are oriented away from one another, and as a consequence, dityrosine formation is more restricted. Graphics generated using PyMol.

Discussion

Dityrosine cross-links represent one of the most important modifications resulting from the oxidation of many proteins under oxidative stress conditions and could affect the protein folding and the structure. Many different models of peptides that contain tyrosine residues have been used to investigate the oxidative modification of tyrosine and formation of dityrosine linkages applying different oxidation system including MCO systems and enzymatic systems [30, 31]. Among these MCO systems, $CuCl_2/H_2O_2$ was the most effective to generate dityrosine and also showed a specificity to produce dityrosine [30, 31]. Dityrosine cross-links were found to increase the stability of *in vitro* amyloid-β and alpha-synuclein [16, 18]. In the current study, two short peptides containing tyrosine residues were used as a model system to generate dityrosine crosslinked amyloid-like fibrils as bionanomaterials. Fluorescence data shows that dityrosine crosslinks formed more effectively in phosphate buffer than HEPES buffer for both HYFNIF and VIYKI peptides. It has been revealed that HEPES buffer is a more suitable buffer in the protein-copper coordination studies, since it does not form ternary complexes with copper ions [29], thus HEPES would not compete with peptide and proteins to bind copper ions. However, it seems from our data that HEPES buffer is less efficient to produce dityrosine. This might be due to the formation of stable $CuCl_2$/peptide complexes in HEPES buffer, which in turn may have less catalytic activity.

Tyrosine fluorescence decreases when the residue goes from a more buried environment to a more solvent-exposed environment [28]. Moreover, it has been reported that in aqueous solvents the fluorescence of tyrosine (that is solvent-exposed) is quenched by the carbonyl group in the peptide bond. However the quenching mechanism is unknown [28]. From the structural model of VIYKI fibril, it is clear that tyrosine residues are located away from the fibril surface (Figure 8) which could result in less fluorescence quenching, whilst in HYFNIF fibrils, tyrosine residues are located on the fibril surface, and this may explain the tyrosine fluorescence quenching.

The potential contribution of other amino acid groups must be taken into account. It has been demonstrated that Histidine residues can form Histidine-bridge in Aβ via coordination with copper ions [32, 33]. In the same manner, we hypothesis that the HYFNIF peptide could coordinate with copper ions to form Histidine-bridges. As a result, this could affect the extent of dityrosine cross-linking. Formation of Histidine-bridged species could lead to more steric hindrance that prevents dityrosine production. Moreover, as explained previously that Histidine residue has a high affinity toward copper ions, forming a stable complex that may have less catalytic activity, yielding less dityrosine.

The structural model of the VIYKI fibrils (Figure 8) suggests that dityrosine cross-links can be formed within and between the fibrils. These results are consistent with other studies conducted on the structural features of HYFNIF and VIYKI fibrils and can be rationalized from structural models which suggest that there is close packing of the aromatic side groups, specifically tyrosine [22]. It seems that peptide side-chain packing in the structure of amyloid-like fibril significantly affects the efficiency of dityrosine cross-link formation.

Conclusion

In this study, the oxidative modification of the two short peptides, HYFNIF and VIYKI, using $CuCl_2/H_2O_2$ oxidation system was explored, and the morphological and conformational changes of these amyloid fibrils over the oxidation process were studied. The results showed that VIYKI fibrils have a greater ability than HYFNIF fibrils to oxidise and produce dityrosine cross-links, and demonstrated that the preformed fibrils could enhance dityrosine formation by bringing two tyrosine residues close enough to cross-link covalently. The results are in good agreement with structural models of HYFNIF and VIYKI fibrils from a previous study, which revealed that phenolic groups of the tyrosine residues in VIYKI fibrils pack closely together and become arranged in a proximity that could make the tyrosine cross-link more favourable. In contrast, the structural model of HYFNIF fibrils suggested that the side chain of the tyrosine residues is further away from each other, and as a consequence, dityrosine formation is more restricted. Dityrosine cross-linked amyloid-like fibrils can be prepared from both HYFNIF and VIYKI peptides and could be utilised as bionanomaterials.

Acknowledgements

The authors would like to thank Mustansiriyah University (www.uomustansiriyah.edu.iq) Baghdad- Iraq for its support in the present work. TEM work was performed at the School of Life Sciences TEM imaging centre at the University of Sussex and we are grateful for Dr. Julian Thorpe for his valuable help. LCS is supported by Alzheimer's Society and Alzheimer's Research UK Southcoast Network. MBM is funded by Alzheimer's Society.

Author contributions

YA planned and carried out the work and wrote the paper. MBM edited and wrote the paper. LCS and AA managed the project and wrote the paper.

References

1. Chen, Q., S. Liang, and G.A. Thouas, Elastomeric biomaterials for tissue engineering. Progress in Polymer Science, 2013. 38(3): p. 584-671.
2. Abbott, R.D. and D.L. Kaplan, Engineering Biomaterials for Enhanced Tissue Regeneration. Current Stem Cell Reports, 2016. 2(2): p. 140-146.
3. Partlow, B.P., et al., Dityrosine Cross-Linking in Designing Biomaterials. ACS Biomaterials Science & Engineering, 2016. 2(12): p. 2108-2121.
4. Shi, R., et al., Recent advances in synthetic bioelastomers. International journal of molecular sciences, 2009. 10(10): p. 4223-4256.
5. Weadock, K., R.M. Olson, and F.H. Silver, Evaluation of collagen crosslinking techniques. Biomater Med Devices Artif Organs, 1983. 11(4): p. 293-318.
6. Andersen, S.O., Cross-Links in Resilin Identified as Dityrosine & Trityrosine. Biochimica Et Biophysica Acta, 1964. 93(1): p. 213-215.
7. Labella, F., et al., Evidence for Dityrosine in Elastin. Biochemical and Biophysical Research Communications, 1967. 26(6): p. 748-&.
8. Raven, D.J., C. Earland, and M. Little, Occurrence of Dityrosine in Tussah Silk Fibroin and Keratin. Biochimica Et Biophysica Acta, 1971. 251(1): p. 96-&.
9. Fujimoto, D., Occurrence of Dityrosine in Cuticlin, a Structural Protein from Ascaris Cuticle. Comparative Biochemistry and Physiology B-Biochemistry & Molecular Biology, 1975. 51(2): p. 205-207.
10. Waykole, P. and E. Heidemann, Dityrosine in Collagen. Connective Tissue Research, 1976. 4(4): p. 219-222.
11. Skaff, O., K.A. Jolliffe, and C.A. Hutton, Synthesis of the side chain cross-linked tyrosine oligomers dityrosine, trityrosine, and pulcherosine. Journal of Organic Chemistry, 2005. 70(18): p. 7353-7363.
12. Kanwar, R. and D. Balasubramanian, Structure and stability of the dityrosine-linked dimer of gamma B-crystallin. Experimental Eye Research, 1999. 68(6): p. 773-784.
13. Bailey, A.J., The chemistry of natural enzyme-induced cross-links of proteins. Amino Acids, 1991. 1(3): p. 293-306.
14. Fetterer, R.H., M.L. Rhoads, and J.F. Urban, Jr., Synthesis of tyrosine-derived cross-links in Ascaris suum cuticular proteins. J Parasitol, 1993. 79(2): p. 160-6.
15. Li, J., B.A. Hodgeman, and B.M. Christensen, Involvement of peroxidase in chorion hardening in Aedes aegypti. Insect Biochem Mol Biol, 1996. 26(3): p. 309-17.
16. Al-Hilaly, Y.K., et al., A central role for dityrosine crosslinking of Amyloid-beta in Alzheimer's disease. Acta Neuropathol Commun, 2013. 1: p. 83.
17. Al-Hilaly, Y.K., et al., The involvement of dityrosine crosslinks in lipofuscin accumulation in Alzheimer's disease. Journal of Physics: Conference Series, 2019. 1294: p. 062107.
18. Al-Hilaly, Y.K., et al., The involvement of dityrosine crosslinking in alpha-synuclein assembly and deposition in Lewy Bodies in Parkinson's disease. Sci Rep, 2016. 6: p. 39171.
19. Wells-Knecht, M.C., et al., Oxidized amino acids in lens protein with age. Measurement of o-tyrosine and dityrosine in the aging human lens. The Journal of biological chemistry, 1993. 268(17): p. 12348-52.
20. Bodaness, R.S. and J.S. Zigler, Jr., The rapid H2O2-mediated nonphotodynamic crosslinking of lens crystallins generated by the heme-undecapeptide from cytochrome C: potential implications for cataractogenesis in man. Biochem Biophys Res Commun, 1983. 113(2): p. 592-7.
21. Maurer-Stroh, S., et al., Exploring the sequence determinants of amyloid structure using position-specific scoring matrices. Nature Methods, 2010. 7(3): p. 237-242.
22. Morris, K.L., et al., Exploring the sequence-structure relationship for amyloid peptides. Biochem J, 2013. 450(2): p. 275-83.

23. Lee, J., et al., Tyrosine-Rich Peptides as a Platform for Assembly and Material Synthesis. Advanced Science, 2019. 6(4): p. 1801255.
24. Cherny, I. and E. Gazit, Amyloids: not only pathological agents but also ordered nanomaterials. Angew Chem Int Ed Engl, 2008. 47(22): p. 4062-9.
25. Sampani, S.I., et al., Zinc–dysprosium functionalized amyloid fibrils. Dalton Transactions, 2019. 48(41): p. 15371-15375.
26. Aubrey, L.D., et al., Quantification of amyloid fibril polymorphism by nano-morphometry reveals the individuality of filament assembly. bioRxiv, 2020.
27. Vadukul, D.M., Y.K. Al-Hilaly, and L.C. Serpell, Methods for Structural Analysis of Amyloid Fibrils in Misfolding Diseases. Methods Mol Biol, 2019. 1873: p. 109-122.
28. Marshall, K.E., et al., Hydrophobic, aromatic, and electrostatic interactions play a central role in amyloid fibril formation and stability. Biochemistry, 2011. 50(12): p. 2061-71.
29. Tougu, V., A. Karafin, and P. Palumaa, Binding of zinc(II) and copper(II) to the full-length Alzheimer's amyloid-beta peptide. Journal of Neurochemistry, 2008. 104(5): p. 1249-1259.
30. Ali, F.E., et al., Metal catalyzed oxidation of tyrosine residues by different oxidation systems of copper/hydrogen peroxide. Journal of Inorganic Biochemistry, 2004. 98(1): p. 173-184.
31. Kato, Y., et al., The hydrogen peroxide/copper ion system, but not other metal-catalyzed oxidation systems, produces protein-bound dityrosine. Free Radical Biology and Medicine, 2001. 31(5): p. 624-632.
32. Smith, D.P., et al., Copper-mediated amyloid-beta toxicity is associated with an intermolecular histidine bridge. J Biol Chem, 2006. 281(22): p. 15145-54.
33. Curtain, C.C., et al., Alzheimer's disease amyloid-beta binds copper and zinc to generate an allosterically ordered membrane-penetrating structure containing superoxide dismutase-like subunits. J Biol Chem, 2001. 276(23): p. 20466-73.